

Forward Neutral Pion Production in $p + p$ and $d + Au$ Collisions at $\sqrt{s_{NN}} = \mathbf{200}$ GeV

J. Adams,² M. M. Aggarwal,²⁸ Z. Ahammed,⁴³ J. Amonett,¹⁹ B. D. Anderson,¹⁹ D. Arkhipkin,¹² G. S. Averichev,¹¹ S. K. Badyal,¹⁸ Y. Bai,²⁶ J. Balewski,¹⁶ O. Barannikova,³¹ L. S. Barnby,² J. Baudot,¹⁷ S. Bekele,²⁷ V. V. Belaga,¹¹ A. Bellingeri-Laurikainen,³⁸ R. Bellwied,⁴⁶ J. Berger,¹³ B. I. Bezverkhny,⁴⁸ S. Bharadwaj,³³ A. Bhasin,¹⁸ A. K. Bhati,²⁸ V. S. Bhatia,²⁸ H. Bichsel,⁴⁵ J. Bielcik,⁴⁸ J. Bielcikova,⁴⁸ A. Billmeier,⁴⁶ L. C. Bland,³ C. O. Blyth,² S-L. Blyth,²⁰ B. E. Bonner,³⁴ M. Botje,²⁶ A. Boucham,³⁸ J. Bouchet,³⁸ A. V. Brandin,²⁴ A. Bravar,³ M. Bystersky,¹⁰ R. V. Cadman,¹ X. Z. Cai,³⁷ H. Caines,⁴⁸ M. Calderón de la Barca Sánchez,¹⁶ O. Catu,⁴⁸ D. Cebra,⁶ Z. Chajecski,²⁷ P. Chaloupka,¹⁰ S. Chattopadhyay,⁴³ H. F. Chen,³⁶ J. H. Chen,³⁷ Y. Chen,⁷ J. Cheng,⁴¹ M. Cherney,⁹ A. Chikanian,⁴⁸ H. A. Choi,³² W. Christie,³ J. P. Coffin,¹⁷ T. M. Cormier,⁴⁶ M. R. Cosentino,³⁵ J. G. Cramer,⁴⁵ H. J. Crawford,⁵ D. Das,⁴³ S. Das,⁴³ M. Daugherty,⁴⁰ M. M. de Moura,³⁵ T. G. Dedovich,¹¹ M. DePhillips,³ A. A. Derevschikov,³⁰ L. Didenko,³ T. Dietel,¹³ S. M. Dogra,¹⁸ W. J. Dong,⁷ X. Dong,³⁶ J. E. Draper,⁶ F. Du,⁴⁸ A. K. Dubey,¹⁴ V. B. Dunin,¹¹ J. C. Dunlop,³ M. R. Dutta Mazumdar,⁴³ V. Eckardt,²² W. R. Edwards,²⁰ L. G. Efimov,¹¹ V. Emelianov,²⁴ J. Engelage,⁵ G. Eppley,³⁴ B. Erasmus,³⁸ M. Estienne,³⁸ P. Fachini,³ J. Faivre,¹⁷ R. Fatemi,²¹ J. Fedorisin,¹¹ K. Filimonov,²⁰ P. Filip,¹⁰ E. Finch,⁴⁸ V. Fine,³ Y. Fisyak,³ K. S. F. Fornazier,³⁵ B. D. Fox,³ J. Fu,⁴¹ C. A. Gagliardi,³⁹ L. Gaillard,² J. Gans,⁴⁸ M. S. Ganti,⁴³ F. Geurts,³⁴ V. Ghazikhanian,⁷ P. Ghosh,⁴³ J. E. Gonzalez,⁷ Y. G. Gorbunov,⁹ H. Gos,⁴⁴ O. Grachov,⁴⁶ O. Grebenyuk,²⁶ D. Grosnick,⁴² S. M. Guertin,⁷ Y. Guo,⁴⁶ A. Gupta,¹⁸ N. Gupta,¹⁸ T. D. Gutierrez,⁶ T. J. Hallman,³ A. Hamed,⁴⁶ J. W. Harris,⁴⁸ M. Heinz,⁴⁸ T. W. Henry,³⁹ S. Heppelmann,²⁹ B. Hippolyte,¹⁷ A. Hirsch,³¹ E. Hjort,²⁰ G. W. Hoffmann,⁴⁰ M. J. Horner,²⁰ H. Z. Huang,⁷ S. L. Huang,³⁶ E. W. Hughes,⁴ T. J. Humanic,²⁷ G. Igo,⁷ A. Ishihara,⁴⁰ P. Jacobs,²⁰ W. W. Jacobs,¹⁶ H. Jiang,⁷ P. G. Jones,² E. G. Judd,⁵ S. Kabana,³⁸ K. Kang,⁴¹ M. Kaplan,⁸ D. Keane,¹⁹ A. Kechechyan,¹¹ V. Yu. Khodyrev,³⁰ B. C. Kim,³² J. Kiryluk,²¹ A. Kisiel,⁴⁴ E. M. Kislov,¹¹ S. R. Klein,²⁰ D. D. Koetke,⁴² T. Kollegger,¹³ M. Kopytine,¹⁹ L. Kotchenda,²⁴ K. L. Kowalik,²⁰ M. Kramer,²⁵ P. Kravtsov,²⁴ V. I. Kravtsov,³⁰ K. Krueger,¹ C. Kuhn,¹⁷ A. I. Kulikov,¹¹ A. Kumar,²⁸ R. Kh. Kutuev,¹² A. A. Kuznetsov,¹¹ R. Lamb,³ M. A. C. Lamont,⁴⁸ J. M. Landgraf,³ S. Lange,¹³ F. Laue,³ J. Lauret,³ A. Lebedev,³ R. Lednický,¹¹ C-H. Lee,³² S. Lehocka,¹¹ M. J. LeVine,³ C. Li,³⁶ Q. Li,⁴⁶ Y. Li,⁴¹ G. Lin,⁴⁸ S. J. Lindenbaum,²⁵ M. A. Lisa,²⁷ F. Liu,⁴⁷ H. Liu,³⁶ J. Liu,³⁴ L. Liu,⁴⁷ Q. J. Liu,⁴⁵ Z. Liu,⁴⁷ T. Ljubicic,³ W. J. Llope,³⁴ H. Long,⁷ R. S. Longacre,³ M. Lopez-Noriega,²⁷ W. A. Love,³ Y. Lu,⁴⁷ T. Ludlam,³ D. Lynn,³ G. L. Ma,³⁷ J. G. Ma,⁷ Y. G. Ma,³⁷ D. Magestro,²⁷ S. Mahajan,¹⁸ D. P. Mahapatra,¹⁴ R. Majka,⁴⁸ L. K. Mangotra,¹⁸ R. Manweiler,⁴² S. Margetis,¹⁹ C. Markert,¹⁹ L. Martin,³⁸ J. N. Marx,²⁰ H. S. Matis,²⁰ Yu. A. Matulenko,³⁰ C. J. McClain,¹ T. S. McShane,⁹ Yu. Melnick,³⁰ A. Meschanin,³⁰ M. L. Miller,²¹ N. G. Minaev,³⁰ C. Mironov,¹⁹ A. Mischke,²⁶ D. K. Mishra,¹⁴ J. Mitchell,³⁴ S. Mioduszewski,³⁹ B. Mohanty,⁴³ L. Molnar,³¹ C. F. Moore,⁴⁰ D. A. Morozov,³⁰ M. G. Munhoz,³⁵ B. K. Nandi,⁴³ S. K. Nayak,¹⁸ T. K. Nayak,⁴³ J. M. Nelson,² P. K. Netrakanti,⁴³ V. A. Nikitin,¹² L. V. Nogach,³⁰ S. B. Nurushev,³⁰ G. Odyniec,²⁰ A. Ogawa,³ V. Okorokov,²⁴ M. Oldenburg,²⁰ D. Olson,²⁰ S. K. Pal,⁴³ Y. Panebratsev,¹¹ S. Y. Panitkin,³ A. I. Pavlinov,⁴⁶ T. Pawlak,⁴⁴ T. Peitzmann,²⁶ V. Perevoztchikov,³ C. Perkins,⁵ W. Peryt,⁴⁴ V. A. Petrov,⁴⁶ S. C. Phatak,¹⁴ R. Picha,⁶ M. Planinic,⁴⁹ J. Pluta,⁴⁴ N. Porile,³¹ J. Porter,⁴⁵ A. M. Poskanzer,²⁰ M. Potekhin,³ E. Potrebenikova,¹¹ B. V. K. S. Potukuchi,¹⁸ D. Prindle,⁴⁵ C. Pruneau,⁴⁶ J. Putschke,²⁰ G. Rakness,^{3,29} R. Raniwala,³³ S. Raniwala,³³ O. Ravel,³⁸ R. L. Ray,⁴⁰ S. V. Razin,¹¹ D. Reichhold,³¹ J. G. Reid,⁴⁵ J. Reinharth,³⁸ G. Renault,³⁸ F. Retiere,²⁰ A. Ridiger,²⁶ H. G. Ritter,²⁰ J. B. Roberts,³⁴ O. V. Rogachevskiy,¹¹ J. L. Romero,⁶ A. Rose,²⁰ C. Roy,³⁸ L. Ruan,²⁰ M. J. Russcher,²⁶ R. Sahoo,¹⁴ I. Sakrejda,²⁰ S. Salur,⁴⁸ J. Sandweiss,⁴⁸ M. Sarsour,³⁹ I. Savin,¹² P. S. Sazhin,¹¹ J. Schambach,⁴⁰ R. P. Scharenberg,³¹ N. Schmitz,²² K. Schweda,²⁰ J. Seger,⁹ I. Selyuzhenkov,⁴⁶ P. Seyboth,²² A. Shabetai,²⁰ E. Shahaliev,¹¹ M. Shao,³⁶ W. Shao,⁴ M. Sharma,²⁸ W. Q. Shen,³⁷ K. E. Shestermanov,³⁰ S. S. Shimanskiy,¹¹ E. Sichtermann,²⁰ F. Simon,⁴³ R. N. Singaraju,⁴³ N. Smirnov,⁴⁸ R. Snellings,²⁶ G. Sood,⁴² P. Sorensen,³ J. Sowinski,¹⁶ J. Speltz,¹⁷ H. M. Spinka,¹ B. Srivastava,³¹ A. Stadnik,¹¹ T. D. S. Stanislaus,⁴² R. Stock,¹³ A. Stolpovsky,⁴⁶ M. Strikhanov,²⁴ B. Stringfellow,³¹ A. A. P. Suaide,³⁵ E. Sugarbaker,²⁷ M. Sumbera,¹⁰ B. Surrow,²¹ M. Swanger,⁹ T. J. M. Symons,²⁰ A. Szanto de Toledo,³⁵ A. Tai,⁷ J. Takahashi,³⁵ A. H. Tang,²⁶ T. Tarnowsky,³¹ D. Thein,⁷ J. H. Thomas,²⁰ A. R. Timmins,² S. Timoshenko,²⁴ M. Tokarev,¹¹ T. A. Trainor,⁴⁵ S. Trentalange,⁷ R. E. Tribble,³⁹ O. D. Tsai,⁷ J. Ulery,³¹ T. Ullrich,³ D. G. Underwood,¹ G. Van Buren,³ N. van der Kolk,²⁶ M. van Leeuwen,²⁰ A. M. Vander Molen,²³ R. Varma,¹⁵ I. M. Vasilevski,¹² A. N. Vasiliev,³⁰ R. Vernet,¹⁷ S. E. Vigdor,¹⁶ Y. P. Vijoyi,⁴³ S. Vokal,¹¹ S. A. Voloshin,⁴⁶ W. T. Waggoner,⁹ F. Wang,³¹ G. Wang,¹⁹ G. Wang,⁴ X. L. Wang,³⁶ Y. Wang,⁴⁰ Y. Wang,⁴¹ Z. M. Wang,³⁶ H. Ward,⁴⁰ J. W. Watson,¹⁹ J. C. Webb,¹⁶ G. D. Westfall,²³ A. Wetzler,²⁰ C. Whitten, Jr.,⁷ H. Wieman,²⁰ S. W. Wissink,¹⁶ R. Witt,⁴⁸ J. Wood,⁷ J. Wu,³⁶ N. Xu,²⁰ Q. H. Xu,²⁰ Z. Xu,³ Z. Z. Xu,³⁶ P. Yepes,³⁴ I-K. Yoo,³² V. I. Yurevich,¹¹ I. Zborovsky,¹⁰ H. Zhang,³ W. M. Zhang,¹⁹

Y. Zhang,³⁶ Z. P. Zhang,³⁶ C. Zhong,³⁷ R. Zoulkarneev,¹² Y. Zoulkarneeva,¹² A. N. Zubarev,¹¹ and J. X. Zuo³⁷

(STAR Collaboration)*

- ¹Argonne National Laboratory, Argonne, Illinois 60439, USA
²University of Birmingham, Birmingham, United Kingdom
³Brookhaven National Laboratory, Upton, New York 11973, USA
⁴California Institute of Technology, Pasadena, California 91125, USA
⁵University of California, Berkeley, California 94720, USA
⁶University of California, Davis, California 95616, USA
⁷University of California, Los Angeles, California 90095, USA
⁸Carnegie Mellon University, Pittsburgh, Pennsylvania 15213, USA
⁹Creighton University, Omaha, Nebraska 68178, USA
¹⁰Nuclear Physics Institute AS CR, 250 68 Řež/Prague, Czech Republic
¹¹Laboratory for High Energy (JINR), Dubna, Russia
¹²Particle Physics Laboratory (JINR), Dubna, Russia
¹³University of Frankfurt, Frankfurt, Germany
¹⁴Institute of Physics, Bhubaneswar 751005, India
¹⁵Indian Institute of Technology, Mumbai, India
¹⁶Indiana University, Bloomington, Indiana 47408, USA
¹⁷Institut de Recherches Subatomiques, Strasbourg, France
¹⁸University of Jammu, Jammu 180001, India
¹⁹Kent State University, Kent, Ohio 44242, USA
²⁰Lawrence Berkeley National Laboratory, Berkeley, California 94720, USA
²¹Massachusetts Institute of Technology, Cambridge, Massachusetts 02139-4307, USA
²²Max-Planck-Institut für Physik, Munich, Germany
²³Michigan State University, East Lansing, Michigan 48824, USA
²⁴Moscow Engineering Physics Institute, Moscow Russia
²⁵City College of New York, New York City, New York 10031, USA
²⁶NIKHEF and Utrecht University, Amsterdam, The Netherlands
²⁷Ohio State University, Columbus, Ohio 43210, USA
²⁸Panjab University, Chandigarh 160014, India
²⁹Pennsylvania State University, University Park, Pennsylvania 16802, USA
³⁰Institute of High Energy Physics, Protvino, Russia
³¹Purdue University, West Lafayette, Indiana 47907, USA
³²Pusan National University, Pusan, Republic of Korea
³³University of Rajasthan, Jaipur 302004, India
³⁴Rice University, Houston, Texas 77251, USA
³⁵Universidade de Sao Paulo, Sao Paulo, Brazil
³⁶University of Science & Technology of China, Hefei 230026, China
³⁷Shanghai Institute of Applied Physics, Shanghai 201800, China
³⁸SUBATECH, Nantes, France
³⁹Texas A&M University, College Station, Texas 77843, USA
⁴⁰University of Texas, Austin, Texas 78712, USA
⁴¹Tsinghua University, Beijing 100084, China
⁴²Valparaiso University, Valparaiso, Indiana 46383, USA
⁴³Variable Energy Cyclotron Centre, Kolkata 700064, India
⁴⁴Warsaw University of Technology, Warsaw, Poland
⁴⁵University of Washington, Seattle, Washington 98195, USA
⁴⁶Wayne State University, Detroit, Michigan 48201, USA
⁴⁷Institute of Particle Physics, CCNU (HZNU), Wuhan 430079, China
⁴⁸Yale University, New Haven, Connecticut 06520, USA
⁴⁹University of Zagreb, Zagreb, HR-10002, Croatia
- (Received 9 February 2006; published 11 October 2006)

Measurements of the production of forward π^0 mesons from $p + p$ and $d + Au$ collisions at $\sqrt{s_{NN}} = 200$ GeV are reported. The $p + p$ yield generally agrees with next-to-leading order perturbative QCD calculations. The $d + Au$ yield per binary collision is suppressed as η increases, decreasing to $\sim 30\%$ of the $p + p$ yield at $\langle \eta \rangle = 4.00$, well below shadowing expectations. Exploratory measurements of azimuthal correlations of the forward π^0 with charged hadrons at $\eta \approx 0$ show a recoil peak in $p + p$

that is suppressed in $d\psi$ Au at low pion energy. These observations are qualitatively consistent with a saturation picture of the low- $x\psi$ gluon structure of heavy nuclei.

DOI: 10.1103/PhysRevLett.97.152302

PACS numbers: 24.85.+p, 13.85.Fb, 13.85.Ni, 25.75.Dw

Little is known about the gluon structure of heavy nuclei [1]. For protons, the gluon parton distribution function ($g\psi$ PDF) is constrained at small $x\psi$ (fraction of nucleon momentum) primarily by scaling violations observed in deep-inelastic lepton scattering (DIS) at the HERA collider [2]. The proton DIS data are accurately described by evolution equations of quantum chromodynamics (QCD) that allow the determination of the $g\psi$ PDF [3]. As $x\psi$ decreases, the $g\psi$ PDF is found to increase from gluon splitting as the partons evolve. At a sufficiently small value of $x\psi$ yet to be determined by experiment, the splitting is expected to become balanced by recombination as the gluons overlap, resulting in gluon saturation [4]. At a given $x\psi$ the density of gluons per unit transverse area is expected to be larger in nuclei than in nucleons; thus, nuclei provide a natural environment in which to search for gluon saturation. Fixed target nuclear DIS experiments are restricted in the kinematics available; they have determined the nuclear $g\psi$ PDF only for $x\psi \approx 0.02$ [1].

Using factorization in a perturbative QCD ($p\psi$ QCD) framework, PDFs and fragmentation functions (FFs) measured in electromagnetic reactions are used to calculate hadronic processes. In $p\psi$ collisions, next-to-leading order (NLO) $p\psi$ QCD calculations quantitatively describe inclusive $\pi\psi$ production over a broad range of pseudorapidity ($\eta\psi = -\ln[\tan(\theta/2)]$) at center-of-mass energy $\sqrt{s} = 200$ GeV [5,6], but not at lower \sqrt{s} [7]. In $p\psi$ QCD, hadroproduction at large $\eta\psi$ from $p\psi$ collisions at $\sqrt{s} = 200$ GeV probes gluons in one proton using the valence quarks of the other, covering a broad distribution of gluon $x\psi$ peaked around 0.02 [8]. Analogously, hadroproduction in the $d\psi$ beam (forward) direction of $d\psi$ Au collisions is sensitive to the gluon structure of the Au nucleus. Quantifying if saturation occurs at RHIC energies is important because the matter created in heavy-ion collisions comes predominantly from the collisions of low- $x\psi$ gluons [9]. Recently, the yield of forward negatively charged hadrons ($h\psi$) in $d\psi$ Au collisions was found to be suppressed relative to $p\psi$ collisions [10]. The suppression is especially significant since isospin effects should reduce $h\psi$ production in $p\psi$ collisions, but not in $d\psi$ Au [8].

Many models try to describe forward hadroproduction from heavy nuclei. In the color glass condensate (CGC) formulation, the low- $x\psi$ gluon density is saturated, resulting in dense color fields that scatter the partons from the deuteron beam [11]. The average gluon- $x\psi$ decreases rapidly with increasing $\eta\psi \approx 10^{-4}$ for pions produced at $\eta\psi = 4$ [12]. Another approach scatters quarks coherently from multiple nucleons, leading to an effective shift in gluon- $x\psi$ [13]. Shadowing models modify the nuclear $g\psi$ PDF in a

standard factorization framework [8,14]. Other models include limiting fragmentation [15], parton recombination [16], and factorization breaking [17].

Additional insight into the particle production mechanism can be gained by analyzing the azimuthal correlations ($\Delta\phi\psi$) of the forward $\pi\psi$ with coincident hadrons. Assuming collinear elastic parton ($2 \rightarrow 2$) scattering, a back-to-back peak at $\Delta\phi\psi = \pi\psi$ is expected, with the rapidity of the recoil particle correlated with $x\psi$ of the struck gluon. In a saturation picture, the quark undergoes multiple interactions through the dense gluon field, resulting in multiple recoil partons instead of a single one [13,18], thereby modifying the $\Delta\phi\psi$ distribution and possibly leading to the appearance of monojets [19].

We present the yields of high energy $\pi\psi$ mesons at forward rapidities from $p\psi$ (Fig. 1) and $d\psi$ Au (Fig. 2) collisions at $\sqrt{s_{NN\psi}} = 200$ GeV. The data are compared with models and with $h\psi$ data at smaller $\eta\psi$. The $\Delta\phi\psi$ distributions of the forward $\pi\psi$ with midrapidity $h\psi$ are presented.

Data were collected by the STAR experiment (Solenoid Tracker at RHIC) at the Brookhaven National Laboratory Relativistic Heavy-Ion Collider (RHIC). At midrapidity, a time projection chamber is used to detect charged particles, while a forward $\pi\psi$ detector (FPD) is used at forward rapidities. In 2002, $p\psi$ collisions were studied with a prototype FPD (PFPD) [5]. In 2003, $p\psi$ collisions were studied with the complete FPD and exploratory measurements were made for $d\psi$ Au collisions.

The luminosity was determined using the rate of coincidences on either side of the interaction region between beam-beam counters (BBC) for $p\psi$ collisions [5] and zero-degree calorimeters for $d\psi$ Au [20]. For $p\psi$ collisions the transverse size of the colliding beams and the number of ions were measured, giving a coincidence cross section of 26.5 ± 0.2 (stat) ± 1.8 (syst) mb [21]. For $d\psi$ Au, the cross section of coincidences was measured to be $(19.5 \pm 1.3)\%$ of the hadronic, $\sigma_{\text{had}}^{\text{Au}}$ [20]. The integrated luminosity for these data was ≈ 350 nb $^{-1}$ (200 $\mu\psi^{-1}$) for $p\psi$ collisions ($d\psi$ Au).

Events required more energy in the calorimeter than from a 15 GeV electron. A BBC coincidence reduces non-collision background but requires an $E\psi$ -independent 10% correction to the yields [5] to account for its efficiency. The energy is calibrated to $\approx 1\%$ from the centroid of the $\pi\psi$ peak in the diphoton invariant mass, $M_{\psi\psi}$ [22]. Monte Carlo simulations with physics backgrounds and the full detector response describe $p\psi$ and $d\psi$ Au data for many variables, e.g., $M_{\psi\psi}$ in Fig. 2 (inset). Jet background is reduced in the FPD by requiring two recon-

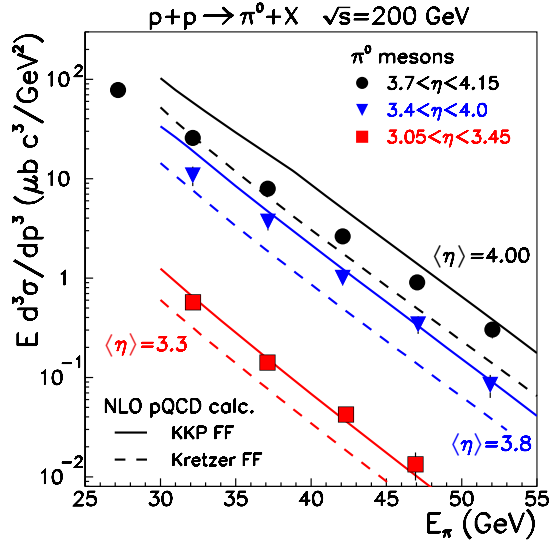


FIG. 1 (color online). Inclusive π^0 cross section for $p\psi$ collisions vs the leading π^0 energy (E_π) averaged over 5 GeV bins at fixed pseudorapidity (η). The error bars combine statistical and point-to-point systematic errors. The curves are NLO p QCD calculations using two sets of fragmentation functions (FF).

structured photons ($N_{\gamma\psi} = 2$), selecting 78% (53%) of events with $E_{\pi\psi} > 25$ GeV and $N_{\gamma\psi} \geq 2$ in $p + p\psi$ ($d + Au$) data. The π^0 detection efficiency is determined in a matrix of $E_{\pi\psi}$ and η from background-corrected simulations. For $d + Au$ it is dominated by the FPD geometrical acceptance and is within 8%–19% of the efficiency in $p\psi$ p .

Inclusive π^0 cross sections for $p + p\psi$ collisions at $\sqrt{s} = 200$ GeV are seen in Fig. 1 at $\langle\eta\rangle = 3.3, 3.8$ [5], and 4.00. Data are in 5 GeV bins, plotted at the average E_π . Data at $\langle\eta\rangle = 3.3$ and 3.8 were taken with the PFPD, where the systematic error increases with $E_{\pi\psi}$ from 10%–26%, dominated by the correction for the jet accompanying the π^0 [5]. Data at $\langle\eta\rangle = 4.00$ were taken with the FPD, where the systematic error is 8%–16%, dominated by the energy calibration [22]. The normalization error is 17% for both $p\psi$ p and $d\psi$ Au , dominated by the absolute η error [22]. The curves are NLO p QCD calculations [23] using CTEQ6M PDFs [24] and equal renormalization and factorization scales of $p_{T\psi} = E_{\pi\psi} / \cosh\eta$. Scale dependence is comparable at $\eta\psi \approx 4$ and $\eta\psi \approx 0$. Theoretical systematic errors, attributed to scale dependence at $\eta\psi \approx 0$ [6], may require further study at large η . The solid and dashed curves use Kniehl-Kramer-Pötter (KKP) [25] and Kretzer [26] fragmentation functions (FFs), respectively. The primary difference between them is the g -to- π FF, which may occur at $p_{T\psi} \lesssim 2$ GeV/ c , where the dominant contribution to π^0 production becomes gg scattering [27]. At $\langle\eta\rangle = 3.3$ and 3.8, the data are consistent with KKP. At $\langle\eta\rangle = 4.00$, the data drop below KKP and approach Kretzer as $p_{T\psi}$ decreases, similar to the trend at $\eta\psi \approx 0$ [6].

The study of effects from possible gluon saturation in a nucleus begins with the inclusive π^0 cross section for $d\psi$ Au

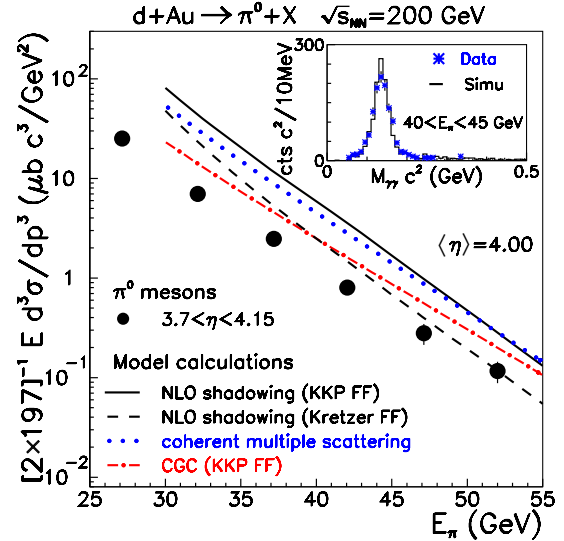


FIG. 2 (color online). Inclusive π^0 cross section per binary collision for $d\psi$ Au collisions, as in Fig. 1. The curves are calculations described in the text. (Inset) Diphoton invariant mass spectrum for data (stars), normalized to simulation (histogram).

Au collisions (Fig. 2). No explicit constraint is placed on the collision centrality. The systematic error is 10%–22%, dominated by the background correction. The solid (dashed) curve is a NLO p QCD calculation using Au PDFs with shadowing [8] and KKP (Kretzer) FFs. The dotted curve is a LO calculation of multiple parton scattering [13], normalized to π^0 data at $\eta\psi \approx 0$ [6]. The dot-dashed curve is a LO calculation convoluting CTEQ5 PDFs and KKP FFs, replacing the hard partonic scattering with a dipole-nucleus cross section to model parton scattering from a CGC in the nucleus [12], normalized to $d + Au \rightarrow h^- + X\psi$ data at $\eta\psi \approx 3.2$ [10]. This model predicts the correct $p_{T\psi}$ dependence but overpredicts the π^0 data by a factor of 2, a factor that could approach unity with use of the Kretzer FF.

The nuclear modification factor is defined as:

$$R_{dAu}^{Y\psi} = \frac{\sigma_{\text{inel}}^{pp\psi}}{\langle N_{\text{bin}} \rangle \sigma_{\text{hadr}}^{dAu}} \frac{E d^3 \sigma / dp^3 (d\psi Au \rightarrow Y\psi X)}{E d^3 \sigma / dp^3 (p + p\psi \rightarrow Y\psi X)} \cdot \psi(1)$$

The inelastic $p + p\psi$ cross section is $\sigma_{\text{inel}}^{pp\psi} = 42$ mb, while $\sigma_{\text{hadr}}^{dAu} = (2.21 \pm 0.09)$ b and the mean number of binary collisions, $\langle N_{\text{bin}} \rangle = 7.5 \pm 0.4$, are from a Glauber model calculation [20]. The prefactor in $R_{dAu}^{Y\psi}$ is equal to the ratio of binary collisions in $p + p\psi$ and $d + Au$, $1/(2 \times 197)$. Figure 3 shows $R_{dAu}^{Y\psi}$ versus $p_{T\psi}$ at $\langle\eta\rangle = 4.00$ with h^- data at smaller $\eta\psi$ [10]. Systematic errors from $p\psi$ $p\psi$ and $d + Au$ are added in quadrature. The normalization error includes the $\langle N_{\text{bin}} \rangle$ error but not the absolute $\eta\psi$ error, since the FPD position was the same for $d + Au$ and $p\psi$ p data.

In the absence of nuclear effects, hard processes scale with the number of binary collisions and $R_{dAu}^{Y\psi} = 1$. At

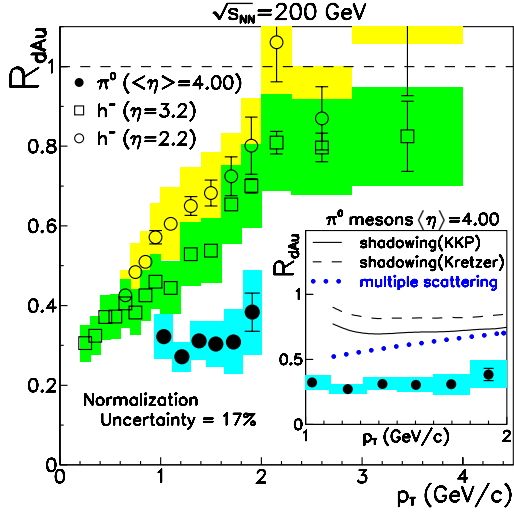


FIG. 3 (color online). Nuclear modification factor (R_{dAu}) for minimum-bias $d\psi$ Au collisions vs transverse momentum (p_T). The solid circles are for π^0 mesons. The open circles and boxes are for negative hadrons [10]. The error bars are statistical, while the shaded boxes are point-to-point systematic errors. (Inset) R_{dAu} for π^0 mesons with the ratio of curves in Figs. 1 and 2.

midrapidity, $R_{dAu}^{h^{\pm}} \geq 1$, with a Cronin enhancement for $p_{T\psi} \gtrsim 2$ GeV/c [10,20]. As $\eta\psi$ increases, R_{dAu} becomes much less than 1. This decrease with $\eta\psi$ is qualitatively consistent with models that suppress the nuclear gluon density [11,13,14,16]. Scaling $R_{dAu}^{h^{\pm}}$ by 2/3 to account for isospin effects on $p\psi$ $p\psi \rightarrow h^{\pm} + X$ [8], $R_{dAu}^{\pi^0}$ is consistent with a linear extrapolation of the scaled $R_{dAu}^{h^{\pm}}$ to $\eta\psi = 4$. The curves in the inset are ratios of the calculations in Figs. 1 and 2. The data lie below all the predictions.

Exploratory measurements of the azimuthal correlations between the forward π^0 and midrapidity h^{\pm} are seen in Fig. 4 for $p + p\psi$ and $d\psi$ Au collisions. The leading charged particle (LCP) analysis picks the track at $|\eta_h| < \psi$ 0.75 with the highest $p_{T\psi} > \psi$ 0.5 GeV/c, and computes $\Delta\phi\psi = \phi_{\pi^0} - \phi_{LCP}$ for each event. The $\Delta\phi\psi$ distributions are normalized by the number of π^0 seen at $\langle\eta\rangle = 4.00$. Correlations near $\Delta\phi\psi = 0$ are not expected since $\eta_{\pi^0} - \eta_{LCP} \approx 4$. The data are fit to a constant plus a Gaussian for the back-to-back peak centered at $\Delta\phi\psi = \pi$. The fit parameters are highly correlated, and their errors are from the full error matrix. The values do not depend on N_γ . The area S under the back-to-back peak is the probability that a LCP is correlated with a forward π^0 . The area $B\psi$ under the constant represents contributions from the underlying event. The total coincidence probability per trigger π^0 is $S + B\psi \approx 0.62(0.90)$ for $p + p\psi$ ($d + Au$), and is constant with E_π . The ratio $S/B\psi$ for $p + p\psi$ does not depend on midrapidity track multiplicity. The peak width has contributions from transverse momentum in hadronization and from momentum imbalance between the scattered partons.

A PYTHIA simulation [28] including detector resolution and efficiencies predicts most features of the $p\psi$ $p\psi$ data

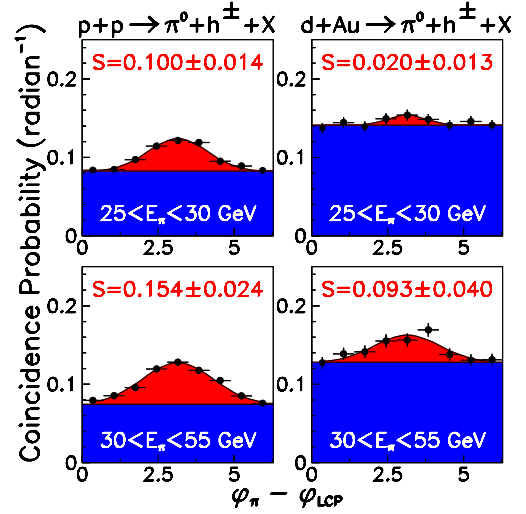


FIG. 4 (color online). Coincidence probability vs azimuthal angle difference between the forward π^0 and a leading charged particle at midrapidity with $p_{T\psi} > \psi$ 0.5 GeV/c. The left (right) column are $p + p\psi$ ($d\psi$ Au) data. The curves are fits described in the text, including the area of the back-to-back peak (S).

[29]. PYTHIA expects $S\psi \approx 0.12$ and $B\psi \approx 0.46$, with the back-to-back peak arising from $2 \rightarrow 2$ scattering, resulting in forward and midrapidity partons that fragment into the π^0 and LCP, respectively. The width of the peak is smaller in PYTHIA than in the data, which may be in part because the predicted momentum imbalance between the partons is too small, as was seen for back-to-back jets at the Tevatron [30].

The back-to-back peak is significantly smaller in $d + Au$ than in $p\psi$ p , qualitatively consistent with the monojet picture in the coherent scattering [13] and CGC [18] models. HIJING [31] uses a model of shadowing for nuclear PDFs. It predicts that the back-to-back peak in $d + Au$ should be similar to $p + p$, with $S\psi \approx 0.08$. The data are not consistent with the HIJING expectation at low E_π .

In conclusion, the inclusive yields of forward π^0 mesons from $p\psi$ $p\psi$ collisions at $\sqrt{s} = 200$ GeV generally agree with NLO p QCD calculations. However, by $\langle\eta\rangle = 4.00$, the spectrum is found to be harder than NLO p QCD, becoming suppressed with decreasing p_T . In $d + Au$ collisions, the yield per binary collision is suppressed with increasing η , decreasing to $\sim 30\%$ of the $p + p\psi$ yield at $\langle\eta\rangle = 4.00$, well below shadowing and multiple scattering expectations, as well as exhibiting isospin effects at these kinematics. The $p_{T\psi}$ dependence of the $d + Au$ yield is consistent with a model which treats the Au nucleus as a CGC. Exploratory measurements of azimuthal correlations of the forward π^0 with charged hadrons at midrapidity show a recoil peak in $p + p\psi$ collisions that is suppressed in $d + Au$ at low E_π , as would be expected for monojet production. These effects are qualitatively consistent with a gluon saturation picture of the Au nucleus, but cannot definitively rule out other interpretations. A systematic

program of measurements, including direct photons and di-hadron correlations over a broad range of $\Delta\eta$, p_T , and \sqrt{s} , is needed to explore the nuclear modifications to particle production. A quantitative theoretical understanding of the observables is needed to facilitate experimental tests of a possible color glass condensate.

We thank the RHIC Operations Group and RCF at BNL, and the NERSC Center at LBNL for their support. This work was supported in part by the HENP Divisions of the Office of Science of the US DOE; the US NSF; the BMBF of Germany; IN2P3, RA, RPL, and EMN of France; EPSRC of the United Kingdom; FAPESP of Brazil; the Russian Ministry of Science and Technology; the Ministry of Education and the NNSFC of China; IRP and GA of the Czech Republic, FOM of the Netherlands, DAE, DST, and CSIR of the Government of India; Swiss NSF; the Polish State Committee for Scientific Research; STAA of Slovakia, and the Korea Science and Engineering Foundation. Support of the RBRC for one of the authors (B.F.) is gratefully acknowledged.

*URL: www.star.bnl.gov

- [1] M. Hirai, S. Kumano, and T.-H. Nagai, Phys. Rev. C **70**, 044905 (2004).
- [2] C. Adloff *et al.*, Eur. Phys. J. C **21**, 33 (2001); S. Chekanov *et al.*, Eur. Phys. J. C **21**, 443 (2001).
- [3] Yu. L. Dokshitzer, Sov. Phys. JETP **46**, 641 (1977); V. N. Gribov and L. N. Lipatov, Sov. J. Nucl. Phys. **15**, 438 (1972); **15**, 675 (1972); G. Altarelli and G. Parisi, Nucl. Phys. **B126**, 298 (1977).
- [4] L. Gribov, E. Levin, and M. Ryskin, Phys. Rep. **100**, 1 (1983); A. Mueller and J. Qiu, Nucl. Phys. **B268**, 427 (1986); L. McLerran and R. Venugopalan, Phys. Rev. D **49**, 3352 (1994); A. Dumitru and J. Jalilian-Marian, Phys. Rev. Lett. **89**, 022301 (2002); E. Iancu, K. Itakura, and D. Triantafyllopoulos, Nucl. Phys. **A742**, 182 (2004).
- [5] J. Adams *et al.*, Phys. Rev. Lett. **92**, 171801 (2004).
- [6] S. S. Adler *et al.*, Phys. Rev. Lett. **91**, 241803 (2003).
- [7] C. Bourrely and J. Soffer, Eur. Phys. J. C **36**, 371 (2004).
- [8] V. Guzey, M. Strikman, and W. Vogelsang, Phys. Lett. B **603**, 173 (2004).
- [9] M. Gyulassy and L. McLerran, Nucl. Phys. **A750**, 30 (2005).
- [10] I. Arsene *et al.*, Phys. Rev. Lett. **93**, 242303 (2004); **91**, 072305 (2003).
- [11] J. Jalilian-Marian, Nucl. Phys. **A748**, 664 (2005); D. Kharzeev, Yu. V. Kovchegov, and K. Tuchin, Phys. Lett. B **599**, 23 (2004); Phys. Rev. D **68**, 094013 (2003); N. Armesto, C. A. Salgado, and U. A. Wiedemann, Phys. Rev. Lett. **94**, 022002 (2005).
- [12] A. Dumitru, A. Hayashigaki, and J. Jalilian-Marian, Nucl. Phys. **A765**, 464 (2006).
- [13] J. Qiu and I. Vitev, Phys. Rev. Lett. **93**, 262301 (2004); Phys. Lett. B **632**, 507 (2006).
- [14] R. Vogt, Phys. Rev. C **70**, 064902 (2004).
- [15] W. Busza and R. Ledoux, Annu. Rev. Nucl. Part. Sci. **38**, 119 (1988).
- [16] R. C. Hwa, C. B. Yang, and R. J. Fries, Phys. Rev. C **71**, 024902 (2005).
- [17] B. Kopeliovich *et al.*, Phys. Rev. C **72**, 054606 (2005); N. Nikolaev and W. Schäfer, Phys. Rev. D **71**, 014023 (2005).
- [18] D. Kharzeev, E. Levin, and L. McLerran, Nucl. Phys. **A748**, 627 (2005).
- [19] D. Kharzeev, Nucl. Phys. **A715**, 35c (2003).
- [20] J. Adams *et al.*, Phys. Rev. Lett. **91**, 072304 (2003).
- [21] A. Drees and Z. Xu, *Proceedings of the IEEE Particle Accelerator Conference, Chicago, IL, 18–22 June 2001* (IEEE, New York, 2001), p. 3120.
- [22] G. Rakness (STAR Collaboration), Nucl. Phys. B, Proc. Suppl. **146**, 73 (2005); D. Morozov (STAR Collaboration), hep-ex/0505024.
- [23] F. Aversa *et al.*, Nucl. Phys. **B327**, 105 (1989); B. Jager *et al.*, Phys. Rev. D **67**, 054005 (2003); D. de Florian *et al.*, *ibid.* **67**, 054004 (2003).
- [24] J. Pumplin *et al.*, J. High Energy Phys. 07 (2002) 012.
- [25] B. A. Kniehl *et al.*, Nucl. Phys. **B597**, 337 (2001).
- [26] S. Kretzer, Phys. Rev. D **62**, 054001 (2000).
- [27] S. Kretzer, Acta Phys. Pol. B **36**, 179 (2005).
- [28] T. Sjöstrand *et al.*, Comput. Phys. Commun. **135**, 238 (2001). Version 6.222 was used.
- [29] A. Ogawa (STAR Collaboration), nucl-ex/0408004.
- [30] V. M. Abazov *et al.*, Phys. Rev. Lett. **94**, 221801 (2005).
- [31] X. N. Wang and M. Gyulassy, Phys. Rev. D **44**, 3501 (1991).